Proceedings of the Eighteenth International Conference on
Civil, Structural and Environmental Engineering Computing
Edited by: P. Iványi, J. Kruis and B.H.V. Topping
Civil-Comp Conferences, Volume 10, Paper 2.3
Civil-Comp Press, Edinburgh, United Kingdom, 2025
ISSN: 2753-3239, doi: 10.4203/ccc.10.2.3

Assessment of Ballast Stability in Multi-Span Simply-Supported Girder Bridges for Increasing Operational Speeds

J. C. Sánchez-Quesada[1], E. Moliner[1], J. Chordà-Monsonís[1], A. Romero[2], P. Galvín[2] and M. D. Martínez-Rodrigo[1]

[1] Department of Mechanical Engineering and Construction, Universitat Jaume I, Castelló de la Plana, Spain
[2] Escuela Técnica Superior de Ingeniería, Universidad de Sevilla, Spain

Abstract

This paper is devoted to the study of track–bridge interaction phenomena in multi–span simply-supported girder bridges for high–speed railway traffic. When one–span numerical models are used to represent the real behavior of a multi–span bridge, the coupling effect exerted by the ballast layer between consecutive, theoretically independent spans is often neglected. This assumption could lead an underestimation of the maximum vibratory levels reached on the platform, which is one of the most restrictive criteria in the design phase of simply-supported bridges. Additionally, the dynamic response of skewed bridges with multi–track decks and open sections under railway loads is more complex than that of straight bridges, due to the participation of three–dimensional modes. Taking two Spanish real bridges as reference, detailed finite element models of these structures are implemented, along with a number of model variants that are used to evaluate the influence of the skew angle, diaphragm configuration, number of spans and their length on the maximum vertical acceleration levels under operating conditions. Whit this aim, this article try to identify those

situations where the use of simplified one–span models could compromise the serviceability limit state of ballasted high speed railway bridges.

Keywords: high–speed railway bridges, track–bridge interaction, skewed girder deck, transverse diaphragms, detailed ballast modelling, vertical acceleration

1 Introduction

Since the opening of the first high–speed railway lines it has become clear that, at certain speeds, railway bridges may experience excessive vertical accelerations at the platform, leading to premature deconsolidation of the ballast layer and the consequent loss of track stability [1,2]. In some cases, this has led a reduction in the operating velocity over these structures or even their temporary closure with the aim of taking corrective actions [1]. Past research has shown that simply–supported girder bridges with short–to–medium spans lengths $(12 - 30\,\mathrm{m})$ are especially critical, due to their low mass and natural frequencies [3]. As a consequence of the problems detected in several high–speed railway bridges, and in order to ensure traffic safety, the maximum vertical acceleration in these structures is limited to $3.5\,\mathrm{m/s^2}$ for ballast tracks [4]. This requirement constitutes one of the most restrictive Serviceability Limit States (SLS) in the design phase of these structures [5,6,7].

The ballast track over a bridge distributes the axle loads from the rails to the structure, acts as a high–frequency filter and introduces a restraining effect at the end sections [8,9,10,11]. Additionally, experimental evidences of load and vibration transfer between consecutive spans which share the continuous ballasted track have been reported [8,9,10,11].

For this reason, the work presented herein analyses the influence of the weak coupling between independent spans exerted by the continuous ballast track on the dynamic response of high–speed railway bridges composed by simply–supported pre–stressed concrete multi–girder decks. The aim of this investigation is to identify conditions under which multi–span models may predict higher responses than typical one–span models on the safe side of the SLS when assessing the maximum deck vertical acceleration under passing trains on ballasted bridges. With this purpose, two Spanish high–speed girder bridges with different span lengths, Jabalón and Arroyo Bracea I bridges, are taken as reference cases for this study. These structures are interesting because they comprise several oblique simply–supported spans. Oblique or skewed bridges, which are frequently founded on Spanish high–speed railway lines [12,13], experience an inherently coupled three-–dimensional dynamic response when traversed by trains [14], especially in multi-–track decks due to the eccentricity of the track. The modelling and updating of this type of bridges is not straight forward, as they are more sensitive to boundary conditions than straight bridges [15]. Detailed finite element (FE) models of the two bridges, which include an explicit representation

of the ballast track and the presence of the transverse diaphragms at the supporting sections of each deck, are implemented. Next, model variants are considered to provide generality to the study and evaluate the influence of the skewness, presence of diaphragms and span length on the restraining effect of the ballast track between adjacent simply–supported spans. Focused in the number of spans included in the bridges numerical models, derivated models of these real structures are considered. In the work presented herein, the influence of the transverse diaphragms installed on the bearing sections, the effect of the obliquity angle and also the influence of the span length is analysed.

2 Baseline: Arroyo Bracea I and Jabalón bridges.

Two existing railway bridges are serve as reference cases in this investigation: the bridges over Bracea and Jabalón rivers, henceforth "Arroyo Bracea I Bridge" and "Jabalón Bridge". Both of them belong to the Madrid–Sevilla high–speed railway line constructed in 1991.

In Figure 1 the technical description of these bridges is depicted. Arroyo Bracea I Bridge presents a skew angle of α = 45° and it is composed by two identical 15.25 m simply–supported spans as illustrated in Figure 1(a). Their decks are composed by a 0.25 m thick, 11.6 m wide, cast–in–place concrete slabs resting over five 1.05 m high pre–stressed concrete I girders equally spaced 2.275 m apart from the slab edges as shown in Figure 1(c). The girders lean on two reinforced concrete abutments and one intermediate pier through laminated rubber bearings. Transverse concrete diaphragms link the deck girders at each span end. Each slab accommodates two ballast tracks with an equal eccentricity of 2.150 m, two sidewalks and handrails. The rails present a UIC60 cross section and rest over rail–pads fixed to monoblock concrete sleepers which are regularly spaced at 0.6 m intervals.

As depicted in Figure 1(b), the Jabalón Bridge crosses the river with an oblique angle of α = 44° using three equal spans of 24.9 m length and 11.6 m width. The outermost spans sections are supported on two external abutments while the inner ones lean on the wall piers. As shown in Figure 1(c), both bridges share the same typology, even though the girder height and slab thickness 2.050 m and 0.30 m, respectively define the Jabalón Bridge For this structure the longitudinal girders are equally spaced apart from the slab edges 2.517m. Additional rubber bearings installed in the external girders restrain the transverse movement of this bridge. Finally, the ballast track layout and components are identical in both cases, and its properties are listed in [16].

In July 2016 and in May 2019 two experimental programs were carried out by the authors to identify Arroyo Bracea I and Jabalón bridges dynamic properties. In both cases, only one span of each bridge was instrumented (shaded spans in Figure 1(a–b)) with vertical accelerometers with nominal sensitivity of 10 V/g and lower frequency limit of approximately 0.1 Hz. As a result of the experimental campaigns five modes

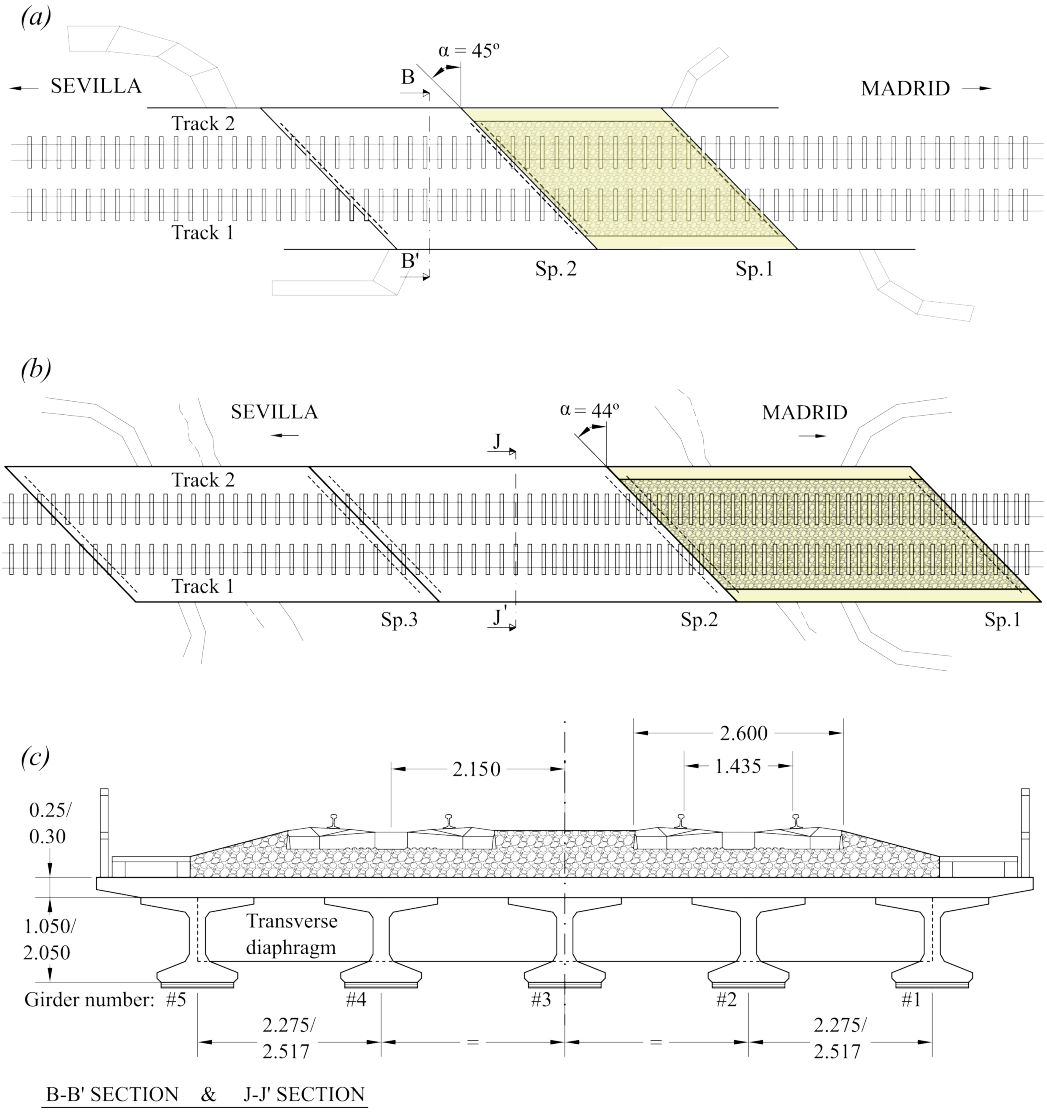

Figure 1: Technical drawings of (a) Arroyo Bracea I Bridge top view; (b) Jabalón Bridge top view; (c) Arroyo Bracea I and Jabalón bridges cross-section B-B' & J-J'.

were identified in each bridge from ambient vibration response by the Stochastic Subspace Identification technique. Their mode shapes (Φ_i^{exp}) are shown in Figure 2 and their associated natural frequencies (f_i^{exp}) are listed in Table 1. This information is used to update the digital twin models of both structures.

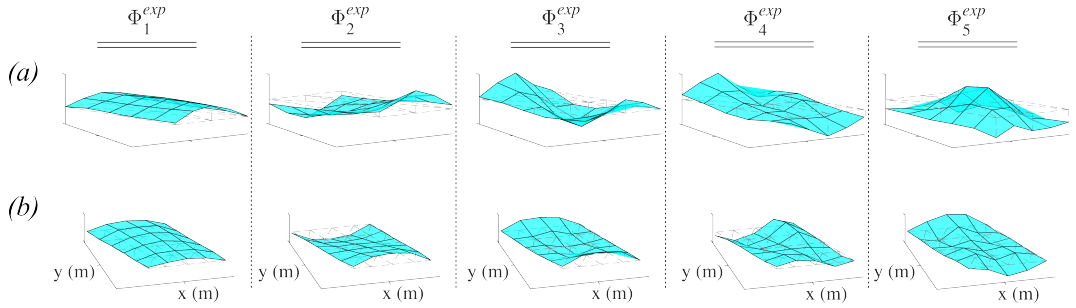

Figure 2: Experimental mode shapes identified for: (a) Bracea Bridge; and (b) Jabalón Bridge.

3 Finite element models of the bridges

In order to develop the digital twins of these structures, two continuous 3D track–bridge FE models are implemented in ANSYS© 2020R2. These digital twins include the whole bridges, considering two or three spans for Arroyo Bracea I and Jabalón bridges respectively. As for the deck, the longitudinal girders, the slab and the transverse diaphragms are meshed with isotropic Mindlin–Reissner shell FE (SHELL181) with 6 degrees of freedom (DOFs) per node. The laminated rubber bearings located under each girder at the supports, are modelled with solid elements (SOLID185) with 3 DOFs per node, considering their real dimensions. The vertical displacement of all the nodes at the bottom surface of the bearings is restrained, therefore ideal fixed boundary conditions are assumed and the flexibility of the piers, abutments neglecting any interaction with the soil. Transverse bearings, only presented in Jabalón bridge, are modelled as discrete elastic springs (COMBIN14).

The ballast bed is discretised with solid FE (SOLID185). Two constitutive models are adopted over the platform: the ballast zone along the transverse joint between adjacent spans or "degraded ballast", shaded in purple in Figure 3, and the rest of ballast or "general ballast", marked in cyan in Figure 3. The degraded ballast is considered as transversely isoropic material, taking into account the possible loss of stiffness due to the relative movement caused by passing trains. This type of material lets the representation of different interlocking mechanisms of the ballast granules in the out–of–plane (vertical) and in the in-plane (horizontal) directions. However, a linear isotropic material behaviour is considered for the non degraded ballast. The sleepers are meshed into SOLID185 FE with elastic isotropic behaviour, while Timoshenko beam elements with 6 DOFs per node (BEAM188) are adopted for the rails. Finally, the rail–pads are simulated as discrete spring-dashpot elements (COMBIN14).

A track extension of 15 m over the embankment on both sides of the bridge models is included. At these extensions, the ballast mesh rests on a subgrade layer, discretised with SOLID185 elements and considering isotropic material properties. The translations are fully restrained for the nodes at the bottom of the subgrade layer. The

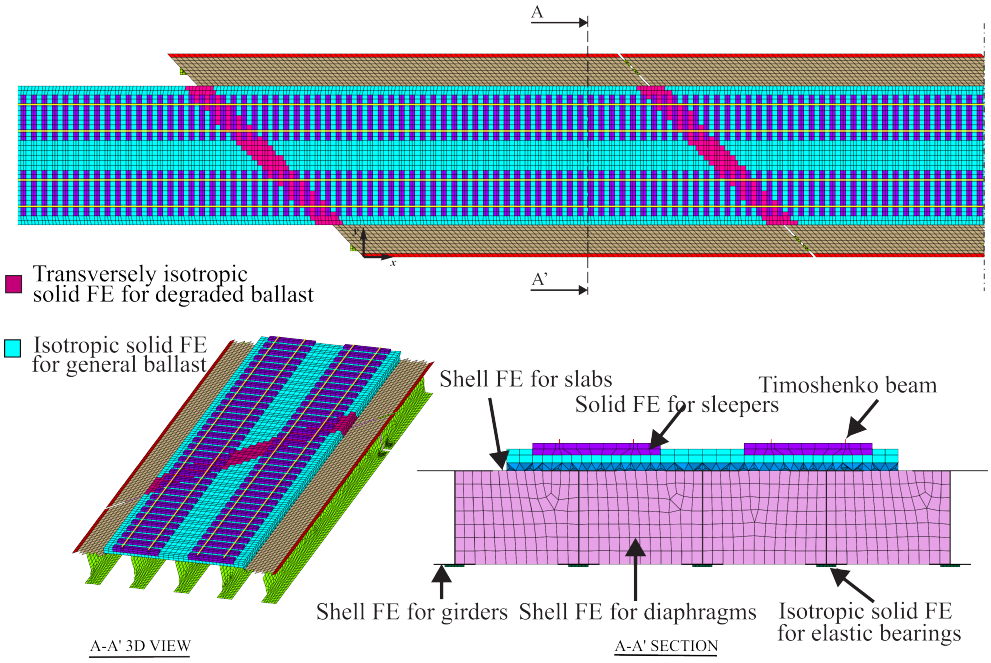

Figure 3: 3D track–bridge FE model. In the view: plan view of half bridge and track extension, 3D detail of deck section and AA' cross section.

self-weight of non–structural elements such as the handrails is included as additional lumped masses (MASS21) uniformly distributed along the two external borders. Additional density is also considered in the sidewalks areas.

bridge	Mode	1	2	3	4	5
Bracea	f_i^{exp} (Hz)	9.25	10.63	12.75	17.92	24.57
	f_j^{num} (Hz)	9.22	11.04	12.67	17.86	-
	$e_{i,j}$ (%)	+0.3	-3.9	+0.6	+0.3	-
	MAC$_{i,j}$ (-)	0.96	0.94	0.95	0.98	-
Jabalón	f_i^{exp} (Hz)	6.30	7.20	9.30	24.00	24.50
	f_j^{num} (Hz)	6.09	7.41	9.88	-	-
	$e_{i,j}$ (%)	+3.4	-2.9	-6.3	-	-
	MAC$_{i,j}$ (-)	0.93	0.95	0.95	-	-

Table 1: Identified experimental frequencies. Numerical frequencies, frequency differences and MAC numbers of the paired modes after calibration.

Table 1 presents the comparison between the experimentally identified vibration modes and those predicted by the calibrated numerical models, in terms of frequency

differences $e_{i,j}$ and $\text{MAC}_{i,j}$ numbers. MAC numbers over 0.93 and frequency differences below $6.29\,\%$ denote enough accuracy. A mesh convergence study was performed to guarantee an accurate prediction of the mode shapes and natural frequencies. Derived finite element models from the aforementioned digital twins are used to determine the influence of the number of spans modelled, their lengths, the skew angle and the diaphragm configurations in the prediction of the maximum response.

4 Results

In this subsection, the weak coupling effect exerted by the track between consecutive simply–supported spans is evaluated in terms of the vertical acceleration predicted by multi–span models. Variants of the previous digital twins are considered to ensure the generality of the study. Models with straight decks $\alpha = (0°)$ and those without extreme transverse diaphragms are also analysed. As a result, the vertical response over 24 derived bridge models is studied, considering: two spans lengths ($L = [15.25, 24.9]$ m); multi–span models up to three spans (NSp. $= [1, 2, 3]$); straight or skewed bridges ($\alpha = [0°, 44°]$); and the presence of transverse diaphragms connected to the slab (FD) or absence of them (ND).

The response of the bridges is calculated in the time domain using Modal Superposition of structural modes up to 30 Hz. According to EN 1991 [16], the adopted modal damping ratios for the longest and shortest span–models are $1.00\,\%$ and $1.33\,\%$, respectively. The constant moving load model HSLM–A from [16] is used to simulate the railway excitation and they cross the bridge models along track 1 from Sevilla to Madrid, see Figure 4. The maximum vertical acceleration is determined over a speed range of $[144 - V_{lim}]$ km/h, for increasing values of V_{lim}. Finally, the maximum bridge vertical acceleration is obtained at different post–process points located underneath girders. For simplicity, the location of the 25 post–process points considered for the one span model is shown in Figure 4. In this figure, "Ai", "Bi", "Ci", "Di" and "Ei" refers to deck's section in the left support, one quarter, mid–span, three–quarters of the span and along the right support, respectively. The lowercase letter "i" refers to girder number (see Figure 1). Extending this nomenclature to multi–span models, "Ai"–"Ei" belong to the first span (entrance of moving loads), "Fi"–"Ji" to the second span and "Ki"–"Oi" to the third span.

Then, the maximum acceleration predicted by the two– or three–span models at each post–process point is presented using the amplification parameter $\bar{a}_{max}$. This parameter is defined as the ratio between the maximum acceleration predicted for the 10 trains at a particular post–process point, and the overall maximum acceleration provided by the single–span model for the same set of trains and velocities. Therefore, when $\bar{a}_{max}$ exceeds unity, the single–span model may be considered non–conservative. Additionally, only in cases where both $\bar{a}_{max} > 1$ and $a_{max} > 3.5\,\text{m/s}^2$, the Serviceability Limit State of the structure is considered to be compromised in terms of vertical acceleration on the platform. These situations constitute critical underestimation of the

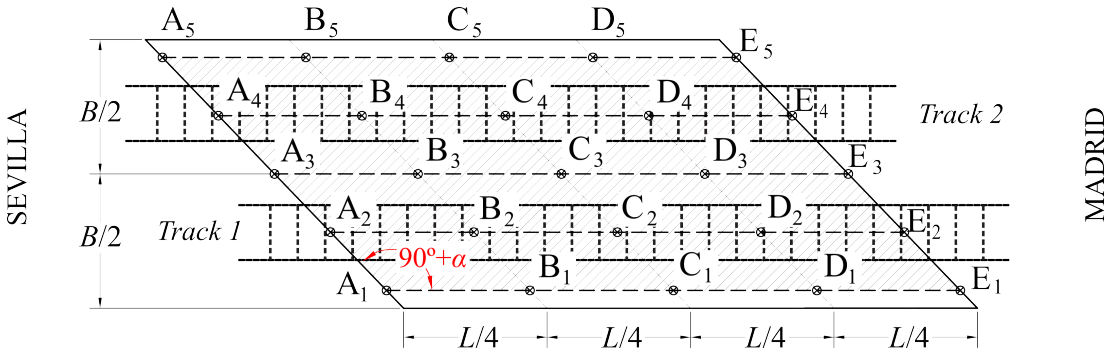

Figure 4: Post–process points in one–span models.

deck's vibrational level and are highlighted in colours in Figures 5 to 8. Furthermore, the lowest speed at which this critical condition is detected, V_{lim0}, is also indicated in the figures.

Figures 5 and 6 show the $\bar{a}_{max}$ ratio at the post–process points within the speed range $[144 - V_{lim}]$ km/h for the two–span and three–span derived models from Arroyo Bracea I Bridge, respectively. It can be concluded that there are situations where the one–span model results non–conservative in the prediction of the maximum acceleration. It is notorious that for the derived models that include the transverse diaphragms at span ends (FD), both with two– and three–span, the overprediction of the acceleration with multi–span models happens starting from higher speeds when compared to the models without diaphragms ($V^{\text{FD}}_{lim0} > V^{\text{ND}}_{lim0}$). In the case of two–span, the maximum amplification of the acceleration reaches 1.25 and occurs in the straight numerical model and when the transverse diaphragms are neglected ($\alpha = 0$ & ND). For the three–span models, there are many more situations where the maximum acceleration is under predicted when only one–span model is used. However, the maximum amplification reached among the three–span models is 1.45, occurring in the skeewed numerical model and when the transverse diaphragms are neglected ($\alpha = 44$ & ND). In general, for both two– and three–span models, the maximum responses are obtained at the border girders in the skewed cases, highlighting the three–dimensional contribution of numerical modes different from longitudinal bending mode.

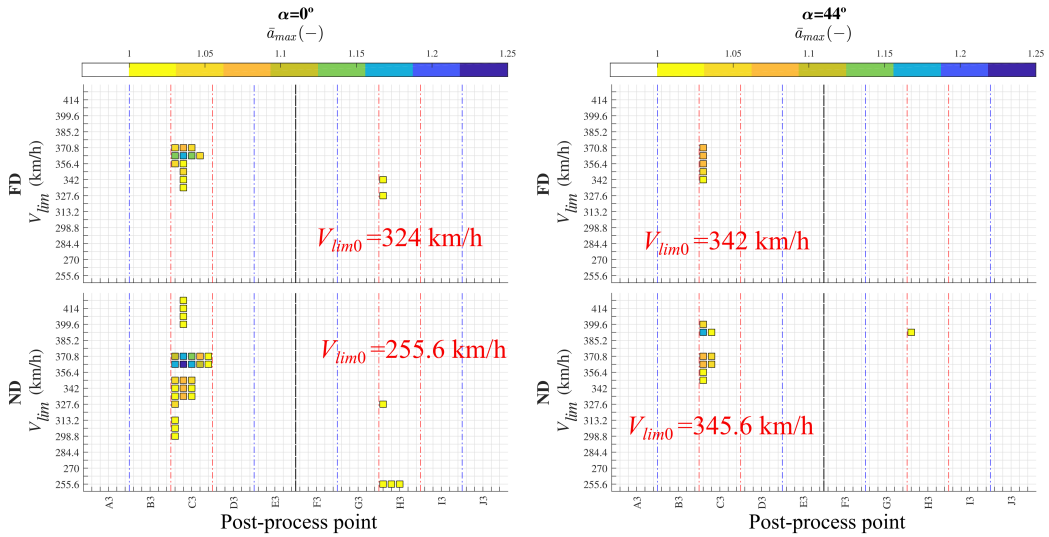

Figure 5: Results over two–spans Arroyo Bracea I Bridge derived models: $\bar{a}_{max}$ at post–process points in the speed range $[144 - V_{lim}]$ km/h for straight and skeewed deck case and for full transverse diaphragms (FD) and absence of diaphragms (ND).

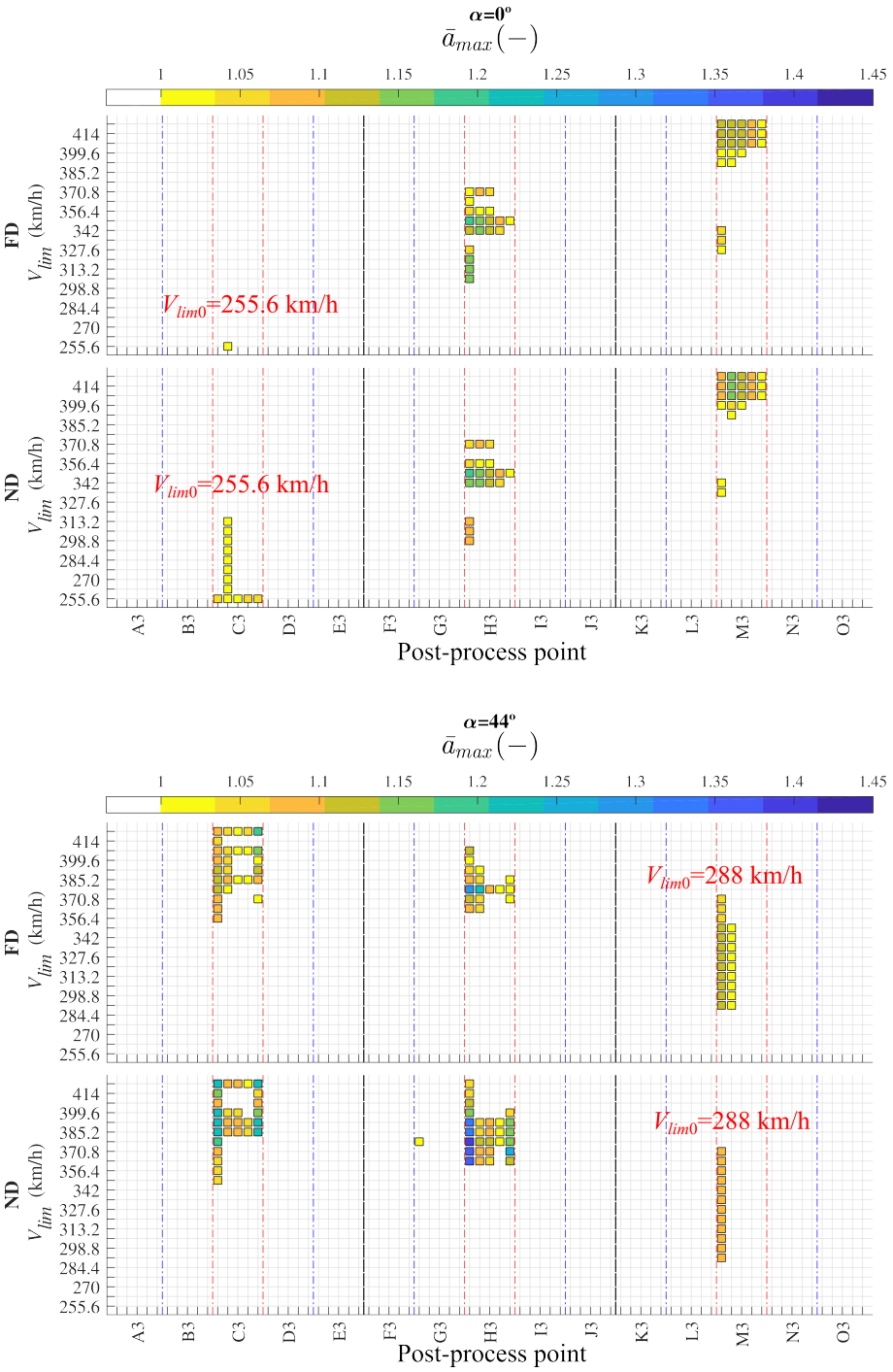

Figure 6: Results over three–spans Arroyo Bracea I Bridge derived models: $\bar{a}_{max}$ at post–process points in the speed range $[144 - V_{lim}]$ km/h for straight and skeewed deck case and for full transverse diaphragms (FD) and absence of diaphragms (ND).

Finally, the derived two– and three–span models from Jabalón Bridge are presented in Figures 7 and 8. The overprediction provided by the multi–span models, with respect to the one–span case, is lower than in the shortest bridges cases. In the case of two–span models, the maximum amplification of acceleration accurs in the skeewed numerical model and when the transverse diaphragms are neglected ($\alpha = 44$ & ND), reaching a value of 1.09 (while in the shorter bridge this value is 1.25). For the three–span models, the maximum overprediction is attained in the straight numerical model and when the transverse diaphragms are considered ($\alpha = 0$ & FD), with a value of 1.35. Once again, the maximum responses are obtained at the border girders in the skewed cases, although with less prominence than in the shorter bridges, denoting the inherent three–dimensional behaviour in the shortest bridges. Finally, it is worth noting that, for the two–span models (both for the shortest and longest bridges), the maximum acceleration generally occurs in the entry span, whereas for the three–span models, this usually takes place in the central span.

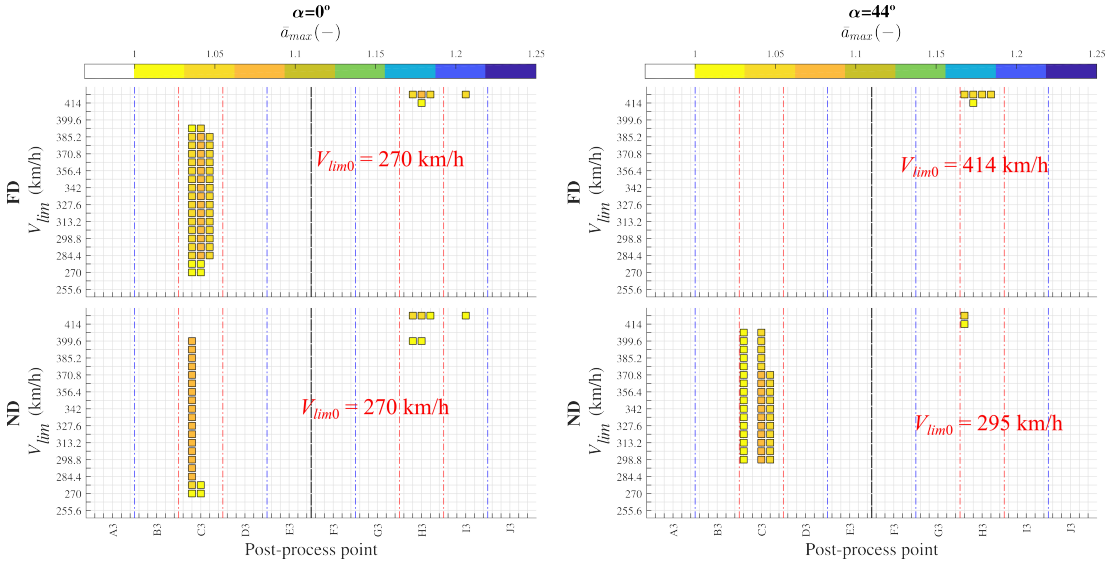

Figure 7: Results over two–spans Jabalón Bridge models: $\bar{a}_{max}$ at post–process points in the speed range $[144 - V_{lim}]$ km/h for straight and skeewed deck case and for full transverse diaphragms (FD) and absence of diaphragms (ND).

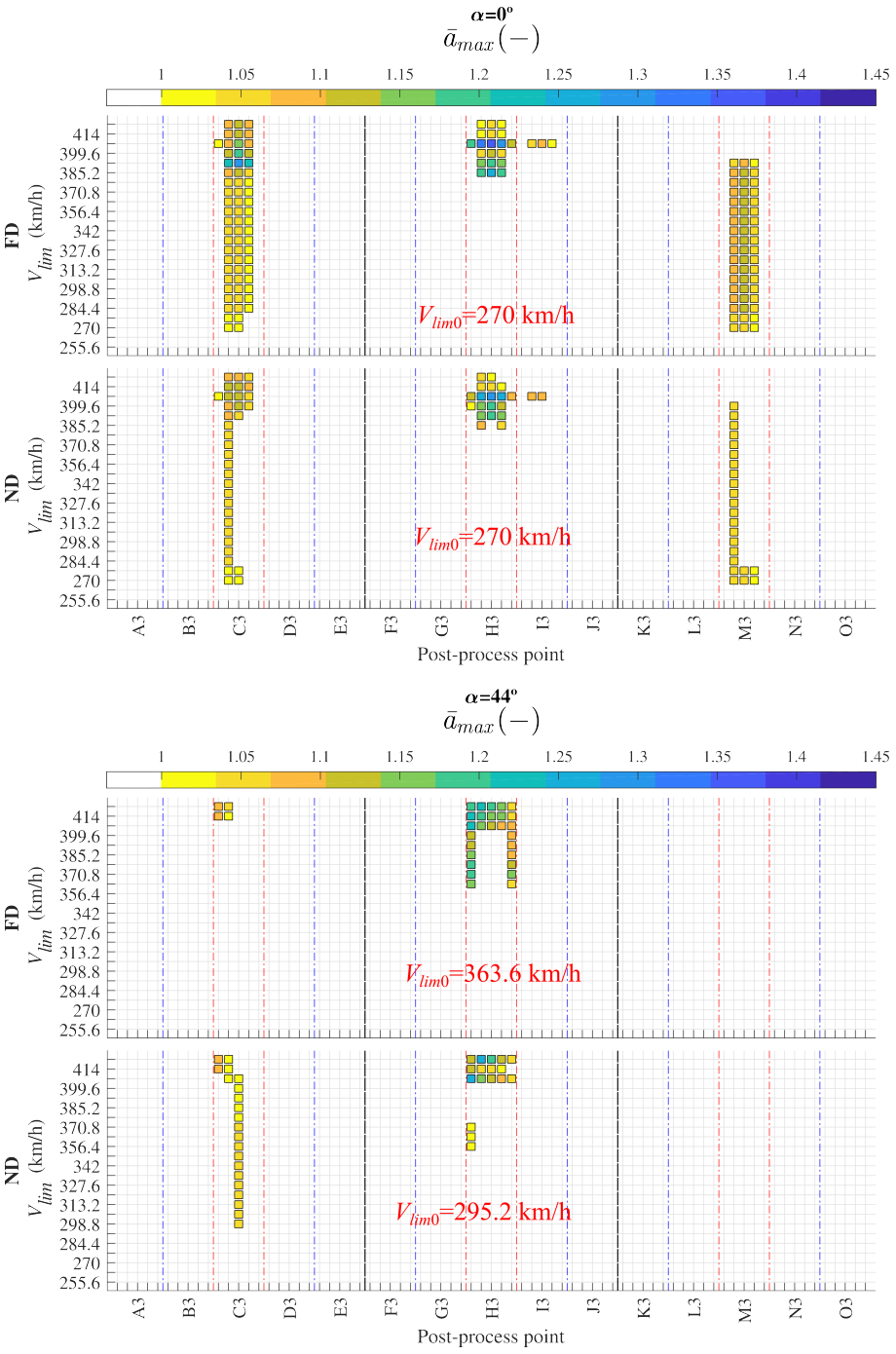

Figure 8: Results over three–spans Jabalón Bridge models: $\bar{a}_{max}$ at post–process points in the speed range $[144 - V_{lim}]$ km/h for straight and skeewed deck case and for full transverse diaphragms (FD) and absence of diaphragms (ND).

5 Conclusions & contributions

There are several situations where the use of one–span numerical models may not be conservative in order to evaluate the SLS of vertical accelerations in simply–supported multi–span girder bridges. Specifically, three–span models tend to exhibit more critical situations than their two–span counterparts. Additionally, the maximum value of $\bar{a}_{max}$ for two–span models usually occurs in the first span in the direction of train travel, while for the three–span models it occurs in the central span. It has been observed that models with shorter spans tend to have a higher $\bar{a}_{max}$ ratio compared to those with longer spans, and in their skeewed variants also a greater influence of three–dimensional modes on the acceleration rate has been detected.

Taking into account the V_{lim} at which the use of one–span models can compromise ballast stability in multi–spans bridges, it has been observed that the vertical response in three–span models is overestimated at lower V_{lim} than in two–span models ($V_{lim0}^{\text{NSp.=3}} < V_{lim0}^{\text{NSp.=2}}$). Moreover, in multi–span models with transverse diaphragms, the critical acceleration overestimation usually occurs at higher V_{lim} values compared to models that neglect the transverse diaphragms ($V_{lim0}^{\text{FD}} > V_{lim0}^{\text{ND}}$).

In general, it can be concluded that neglecting the weak coupling effect of the ballasted track may lead to non–conservative predictions of the maximum acceleration under passing trains in simply–supported multi–span bridges, specially at high speeds, and that this effect may be more important in the case of short spans, where relevant differences have been detected.

Nevertheless, some of the aforementioned conclusions may be model dependent. In this article, the implemented track model allows the transmission of both traction and compression forces between the sleepers and the ballast. Further research is required in this regard to accurately quantify the extent of this effect for engineering purposes, using more realistic ballast models.

Acknowledgements

The authors acknowledge the financial support provided by the Spanish Ministry of Science (PID2022–138674OB–C2), Andalusian Ministry of University, Research and Innovation (PROYEXCEL 00659) and Andalusian Scientific Computing Centre.

This project has received funding from the Europe's Rail Joint Undertaking under Horizon Europe research and innovation programme under grant agreement No. 101121765 (HORIZON-ER-JU-2022-ExplR-02). Views and opinions expressed are however those of the author(s) only and do not necessarily reflect those of the European Union or Europe's Rail Joint Undertaking. Neither the European Union nor the granting authority can be held responsible for them.

References

[1] ERRI, "Rail Bridges for Speeds $>$ 200km/h. Final Report Part A: Synthesis of the results of D 214 research Part B: Proposed UIC Leaflet (D-214/RP9)", 2000.

[2] T. Ishibashi, "Shinkansen structures in Japan", Paper presented at the Workshop on Bridges for High–Speed railways, 2004.

[3] L. Frýba, "Dynamic behaviour of bridges due to high speed trains", bridges for high–speed railways, 2008.

[4] CEN, "Basis of structural design and geotechnical design–Annex A2: Application for bridges (EN 1990:2023)", 2023.

[5] J.M. Goicolea–Ruigómez, "Service limit states for railway bridges in new design codes IAPF and Eurocodes", 2008.

[6] J. Nasarre, "Serviceability limit states of railway bridges", 2004.

[7] B. Pring, A.M. Ruiz–Teran, "Modelling traffic action in high-speed railway bridges", Proceedings of the Institution of Civil Engineers – Bridge Engineering, 173(3), 123—142, 2020.

[8] C. Rigueiro, C. Rebelo, L. Simões da Silva, "Influence of ballast models in the dynamic response of railway viaducts", J Sound Vib, 329 (15), pp. 3030-3040, 2010.

[9] C. Rebelo, M. Heiden, M. Pircher, L. Simões da Silva, "Vibration measurements on existing single–span concrete railway viaducts in Austria", 6th International Conference on Structural Dynamics, 2005.

[10] C. Rebelo, L. Simões da Silva, C. Rigueiro, M. Pircher, "Dynamic behaviour of twin single–span ballasted railway viaducts – Field measurements and modal identification", Eng Struct, 30 (9), pp. 2460-2469, 2008.

[11] C. Rigueiro, C. Rebelo, L. Simões da Silva, "Vibration of the railway track–viaduct system under moving vehicles taking into account the interaction effect", International Conference on Noise and Vibration Engineering (ISMA2006), 2006.

[12] J.J. Soriano, "Dynamic study of accelerations in underpasses of high–speed lines", Master's thesis from E.T.S.I. Caminos, Canales y Puertos, UPM, Spain, 2016.

[13] E. Barrios, "Dynamic study of isostatic and short–span railway bridges. High–speed line Madrid — Zaragoza — Barcelona — French border", Master's thesis from E.T.S.I. Caminos, Canales y Puertos, UPM, Spain, 2017.

[14] K. Nguyen, C. Velarde, J.M. Goicolea, "Analytical and simplified models for dynamic analysis of short skew bridges under moving loads", Advances in Structural Engineering, 22(9), 2076-–2088, 2019.

[15] P. Ryjáček, M. Polák, T. Plachý, J. Kašpárek, "The dynamic behaviour of the extremely skewed railway bridge "Oskar"", Procedia Structural Integrity, 5, 1051—1056, 2017.

[16] CEN, "Eurocode 1: Actions on Structures – Part 2: Traffic loads on bridges and other civil engineering works (EN 1991-2:2023)", 2023.